telluro)acetylene. To a solution of sodium borohydride (1.9 g, 50 mmol) in ethanol (100 mL) in a 500-mL three-necked flask equipped with a dropping funnel, reflux condenser, and nitrogen inlet were added 2 mL of a solution prepared from phenyl(butyltelluro)acetylene (11.4 g, 40 mmol) and ethanol (40 mL). The reaction mixture was stirred and refluxed until the red color had disappeared and the gas evolution had ceased. Then the remaining ethanolic solution of phenyl(butyltelluro)acetylene (38 mL) was added dropwise. The rate of addition must be carefully adjusted to control foaming. When all the solution had been added, the mixture was refluxed for 3 h, cooled to room temperature, then treated with water (3 mL), diluted with diethyl ether (150 mL), and washed with brine (3 × 100 mL). The organic layer was separated, dried over anhydrous magnesium sulfate, and filtered. The filtrate was evaporated in a rotatory evaporator at 20 mmHg and the residue purified by flash chromatography on silica gel with hexane as mobile phase. The product (10.5 g, 92% yield) gave an ^{1}H NMR spectrum identical with published data.[29]

(*Z*)-1-Phenyl-1-hydroxy-3-phenylprop-2-ene from (*Z*)-1-(Butyltelluro)-2-phenylethene. To (*Z*)-1-butyltelluro-2-phenylethene (0.288 g, 1 mmol) in THF (3 mL) at −78 °C under nitrogen was added dropwise *n*-BuLi (0.67 mL, 1.5 M in hexane). The mixture was stirred at this temperature for 30 min, warmed to 0 °C, and then treated with benzaldehyde (0.106 g, 1 mmol). The mixture was stirred at 0 °C for 30 min, diluted with diethyl ether (40 mL), and washed with brine (4 × 15 mL). The organic layer was separated, dried over anhydrous magnesium sulfate, and filtered. The filtrate was evaporated in a rotatory evaporator at 20 mmHg. The product was purified by column chromatography on silica gel. Hexane eluted dibutyl telluride and ethyl acetate, the product (0.176 g, 85% yield). ^{1}H NMR ($CDCl_3$): δ 2.40 (s, 1 H); 5.57 (d, J = 9.2 Hz, 1 H), 5.89 (dd, J = 9.2, J = 11.0 Hz, 1 H), 6.64 (d, J = 11.0 Hz, 1 H), 2.2–7.3 (m, 10 H). IR (film): 3351, 1601 cm^{-1}.

(*Z*)-Phenyl-1-hydroxy-3-phenylprop-2-ene from (*Z*)-Bis-(2-phenylethenyl) Telluride. To a solution of (*Z*)-bis(2-phenylethenyl) telluride (0.334 g, 1 mmol) in THF (4 mL) at −78 °C under nitrogen was added dropwise a solution of *n*-BuLi (1.34 mL, 2 mmol, 1.5 M solution in hexane). After 40 min of stirring at this temperature, benzaldehyde (212 mg, 2 mmol) was added. The reaction mixture was allowed to reach room temperature (30 min), then diluted with ethyl acetate (40 mL), and washed with brine (4 × 15 mL). The organic layer was separated, dried with anhydrous magnesium sulfate, and filtered. The filtrate was evaporated in a rotatory evaporator at 20 mmHg. The residue was purified by column chromatography on silica gel. Elution with hexane removed dibutyl telluride, and elution with ethyl acetate yielded the product (334 mg, 80% yield).

Reaction of Sulfur Dioxide with the Unsaturated Triosmium–Platinum Clusters $Os_3Pt(\mu\text{-}H)_2(CO)_{10}(PR_3)$ (R = c-C_6H_{11}, C_6H_5). X-ray Crystal Structure of $Os_3Pt(\mu\text{-}H)_2(\mu\text{-}SO_2)(CO)_{10}(PCy_3)$

Paul Ewing and Louis J. Farrugia*

Department of Chemistry, The University, Glasgow G12 8QQ, U.K.

Received October 17, 1988

Treatment of $Os_3Pt(\mu\text{-}H)_2(CO)_{10}(PR_3)$ (**1a**, R = Cy) in CH_2Cl_2 with excess SO_2 at ambient temperatures affords reasonable isolated yields of the 60-electron adduct $Os_3Pt(\mu\text{-}H)_2(\mu\text{-}SO_2)(CO)_{10}(PCy_3)$ (**3**), which has been characterized by multinuclear NMR and a single-crystal X-ray structure. Crystal data for **3**: monoclinic; space group $P2_1/n$; a = 13.254 (2), b = 15.893 (5), c = 17.079 (2) Å; β = 101.073 (9)°; V = 3531 (1) Å^3; Z = 4; final R (R_w) values 0.027 (0.036) for 4622 independent observed data ($I > 3.0\sigma(I)$). Complex **3** contains a tetrahedral Os_3Pt core with the SO_2 ligand bridging an Os–Os edge (Os(1)–Os(3) = 2.988 (1) Å). The two hydride ligands bridge the Os(2)–Os(3) edge (2.976 (1) Å) and the Pt–Os(2) vector (2.906 (1) Å). NMR studies on the reaction at 195 K suggest that the initially formed product is a butterfly Os_3Pt species with a Pt-bound SO_2 ligand. This product is unstable at ambient temperatures and rapidly converts to a mixture of complexes including **3**. Complex **3** exists as two isomers in solution, and in the absence of excess SO_2 cluster degradation readily occurs. Treatment of (**1b**, R = Ph) with SO_2 at ambient temperatures affords the analogous complex $Os_3Pt(\mu\text{-}H)_2(\mu\text{-}SO_2)(CO)_{10}(PPh_3)$ which in solution exists primarily as an isomer containing equivalent Os–Os edge-bridged hydrides.

Introduction

Numerous kinetic studies on the ligand substitution reactions of small homometallic carbonyl clusters have shown that both associative and dissociative mechanisms operate and that their relative rates depend both on the metal atom and on the nature of the ancilliary ligands.[1-4] Although fewer kinetic studies have been carried out on heterometallic clusters, it is well-known that these species may display metal site specificity in their substitution reactions with donor ligands.[5] In this context the re-

(1) (a) Dahlinger, K.; Falcone, F.; Poë, A. J. *Inorg. Chem.* **1986**, *25*, 2654. (b) Poë, A. J.; Sekhar, V. C. *Ibid.* **1985**, *24*, 4376. (c) Ambwani, B.; Chawla, S.; Poë, A. J. *Ibid.* **1985**, *24*, 2635.

(2) (a) Darensbourg, D. J.; Baldwin-Zusche, B. J. *J. Am. Chem. Soc.* **1982**, *104*, 3906. (b) Darensbourg, D. J.; Incorvia, M. J. *Inorg. Chem.* **1980**, *19*, 2585. (c) Darensbourg, D. J.; Zalewski, D. J. *Ibid.* **1984**, *23*, 4382. (d) Darensbourg, D. J.; Zalewski, D. J. *Organometallics* **1985**, *4*, 92.

(3) (a) Sonnenberger, D.; Atwood, J. D. *Inorg. Chem.* **1981**, *20*, 3243. (b) Sonnenberger, D.; Atwood, J. D. *Organometallics* **1982**, *1*, 694.

(4) (a) Bavaro, L. M.; Montangero, P.; Keister, J. B. *J. Am. Chem. Soc.* **1983**, *105*, 4977. (b) Rahman, Z. A.; Beanan, L. R.; Bavaro, L.; Modi, S. P.; Keister, J. B.; Churchill, M. R. *J. Organomet. Chem.* **1984**, *263*, 75. (c) Bavaro, L. M.; Keister, J. M. *Ibid.* **1985**, *287*, 357. (d) Dalton, D. M.; Barnett, D. J.; Duggan, T. P.; Keister, J. B.; Malik, P. T.; Modi, S. P.; Shaffer, M. R.; Smesko, S. A. *Organometallics* **1985**, *4*, 1854.

(5) Matsuzaka, H.; Kodama, T.; Uchida, Y.; Hidai, M. *Organometallics* **1988**, *7*, 1608 and ref 7 therein.

0276-7333/89/2308-1665$01.50/0

activity of electronically or coordinatively unsaturated clusters is of particular interest, since such complexes should react with donor ligands exclusively by an associative route. A knowledge of the nature and localization of the LUMO may allow a rationalization of any regioselectivity of nucleophilic attack.

We have been interested in the reactivity of the unsaturated 58-electron heteronuclear clusters *tetrahedro*-$Os_3Pt(\mu\text{-}H)_2(CO)_{10}(PR_3)$ (**1**)[6] which have been shown[7-9] to react readily with 2-electron donor ligands affording the saturated 60-electron adducts $Os_3Pt(\mu\text{-}H)_2(CO)_{10}(PR_3)(L)$ (**2**). An intriguing feature of these adducts is that they may either adopt a butterfly metal core as for **2a** (R = Cy; L = CO)[8] or **2b** (R = Ph; L = PPh_3)[7] or a tetrahedral core as for **2c** (R = Cy; L = μ-CH_2)[8] or **2d** (R = Cy; L = 2 μ-H)[8].

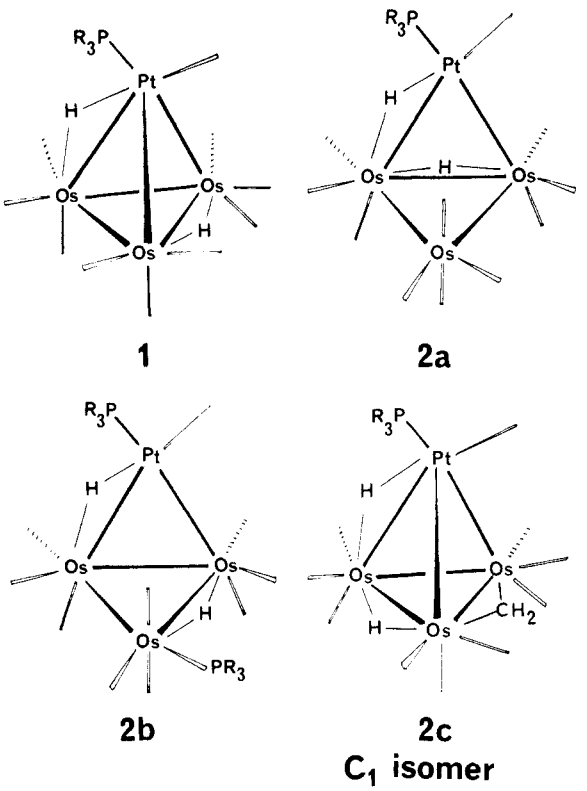

Recently reported[10] extended Hückel MO calculations on **1** indicate that the low-lying LUMO is localized along the hydride-bridged Os–Os bond and is strongly Os–Os antibonding. Structural studies on the 58-electron clusters **1a** (R = Cy),[6] $Os_3Pt(\mu\text{-}H)_2(CO)_9(CNCy)(PCy_3)$,[9] and $[Os_3Pt(\mu\text{-}H)_3(CO)_{10}(PCy_3)]^+BF_4^-$[11] all show an unusually short Os(μ-H)Os vector (2.747 (1)–2.789 (1) Å, *mean* 2.76 Å), while in the 60-electron saturated adducts[7-9] the corresponding bond lengths (2.869 (1)–3.043 (2) Å, *mean* 2.97 Å) are all longer and of normal dimensions. These results are consistent with the population of an orbital of Os–Os antibonding character in going from the 58- to the 60-electron species and suggest a localization of unsaturation about this Os–Os bond. The known structures of the adducts **2a–c** all contain the incoming ligand L bonded to Os atoms, and in view of this evidence, it seems a reasonable supposition that nucleophilic attack under orbital control occurs at these Os centers. The EHMO calculations indicate however that if charge considerations are paramount, nucleophilic attack may occur at the Pt atom since this carries a slight positive charge of +0.52, compared with negative charges of ca. −1.7 at the Os centers. The calculations[10] also suggested that a tetrahedral Os_3Pt arrangement in the adducts **2** could be stabilized by bridging ligands L having frontier orbitals resembling those of the CH_2 unit, i.e., a σ-donor and a single π-acceptor function of suitable energy.

Chart I

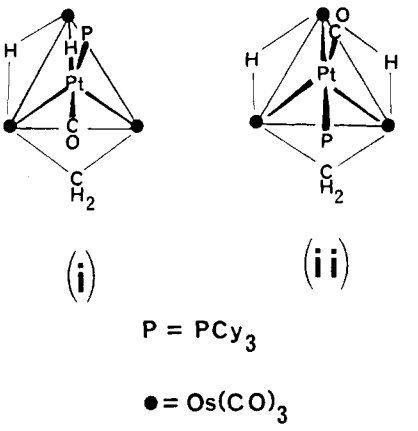

The methylene adduct **2c** exists as a mixture of two isomers, both containing a tetrahedral Os_3Pt skeleton but differing in the disposition of the hydride ligands and the orientation of the $Pt(CO)(PCy_3)$ unit relative to the Os_3 triangle.[8] The red C_1 isomer (i, Chart I) has two inequivalent hydrides, one bridging an Os–Os and the other an Os–Pt edge, with the phosphine eclipsing the Pt(μ-H)Os edge. The yellow C_s isomer (ii) has two hydrides bridging equivalent Os–Os edges, and the $Pt(CO)(PCy_3)$ unit is rotated 180° relative to the Os_3 triangle such that the CO ligand is now eclipsing the Pt–Os edge. The two isomers are in equilibrium, with the red species being the thermodynamically favored product.[8] In view of the known similarity between the frontier orbitals of SO_2 and CH_2,[12] we have examined the reaction of complexes **1a** (R = Cy) and **1b** (R = Ph) with SO_2 to determine whether analogous products are formed. The HOMO ($4a_1$, σ donor) and LUMO ($2b_1$, π acceptor) of sulfur dioxide[12] provide suitable symmetry matches for the HOMO and LUMO, respectively, of **1**.

Results and Discussion

Reaction of Complex 1a with SO_2 at 298 K. Saturation of a solution of **1a** in CH_2Cl_2 with SO_2 at 298 K resulted in a rapid color change from dark green to red. Addition of hexane and overnight cooling afforded the dark red crystalline complex $Os_3Pt(\mu\text{-}H)_2(\mu\text{-}SO_2)(CO)_{10}(PCy_3)$ (**3**) in reasonable yields. ^1H NMR studies (discussed in detail below) show that this species is the major product formed and that it is reasonably stable in solution only in the presence of excess SO_2. An IR spectrum (KBr disk) of complex **3** shows two bands at 1040 and 1195 cm^{-1} in the S–O stretching region, which are typical[13] for μ-SO_2 ligands. A ^1H NMR spectrum of **3** obtained immediately after dissolution of a pure crystalline sample[14] in CD_2Cl_2

(6) Farrugia, L. J.; Howard, J. A. K.; Mitrprachachon, P.; Stone, F. G. A.; Woodward, P. *J. Chem. Soc., Dalton Trans.* **1981**, 155.
(7) Farrugia, L. J.; Howard, J. A. K.; Mitrprachachon, P.; Stone, F. G. A.; Woodward, P. *J. Chem. Soc., Dalton Trans.* **1981**, 162.
(8) Farrugia, L. J.; Green, M.; Hankey, D. R.; Murray, M.; Orpen, A. G.; Stone, F. G. A. *J. Chem. Soc., Dalton Trans.* **1985**, 177.
(9) Ewing, P.; Farrugia, L. J. *Organometallics* **1988**, *7*, 871.
(10) Ewing, P.; Farrugia, L. J. *New J. Chem.* **1988**, *12*, 409.
(11) Ewing, P.; Farrugia, L. J.; Rycroft, D. S. *Organometallics* **1988**, *7*, 859.
(12) Ryan, R. R.; Kubas, G. J.; Moody, D. C.; Eller, P. G. *Struct. Bonding (Berlin)* **1981**, *46*, 47.
(13) Kubas, G. J. *Inorg. Chem.* **1979**, *18*, 182.

Table I. Final Positional Parameters (Fractional Coordinates) with Esd's in Parentheses and Isotropic Thermal Parameters (Equivalent Isotropic Parameters (U_{eq}) for Anisotropic Atoms) for $Os_3Pt(\mu\text{-}H)_2(\mu\text{-}SO_2)(CO)_{10}(PCy_3)$ (3)[a]

	x/a	y/b	z/c	U_{eq}, Å^2
Os(1)	0.60565 (3)	0.18674 (2)	0.77234 (2)	0.025
Os(2)	0.76513 (3)	0.30264 (2)	0.81582 (2)	0.025
Os(3)	0.56537 (3)	0.36653 (2)	0.72543 (2)	0.023
Pt	0.68748 (3)	0.26012 (2)	0.64971 (2)	0.022
S	0.49627 (18)	0.28582 (14)	0.81741 (14)	0.033
P	0.80915 (17)	0.26150 (13)	0.56543 (12)	0.021
O(1)	0.4153 (7)	0.0940 (5)	0.6844 (5)	0.075
O(2)	0.7585 (6)	0.0602 (4)	0.7277 (4)	0.054
O(3)	0.6268 (7)	0.0975 (5)	0.9320 (5)	0.072
O(4)	0.9224 (7)	0.4446 (5)	0.8549 (5)	0.070
O(5)	0.9272 (7)	0.1663 (5)	0.8493 (6)	0.076
O(6)	0.7384 (7)	0.2876 (5)	0.9886 (4)	0.064
O(7)	0.6642 (7)	0.4765 (4)	0.6120 (4)	0.069
O(8)	0.3730 (6)	0.3378 (5)	0.6007 (4)	0.054
O(9)	0.4790 (6)	0.5203 (4)	0.7929 (4)	0.056
O(10)	0.5137 (6)	0.1906 (6)	0.5284 (5)	0.064
O(11)	0.5212 (5)	0.3127 (4)	0.8996 (4)	0.045
O(12)	0.3860 (5)	0.2678 (4)	0.7895 (4)	0.049
C(1)	0.4848 (9)	0.1286 (6)	0.7151 (6)	0.045
C(2)	0.7033 (8)	0.1122 (6)	0.7386 (5)	0.037
C(3)	0.6174 (8)	0.1308 (7)	0.8720 (6)	0.045
C(4)	0.8647 (8)	0.3936 (6)	0.8372 (6)	0.041
C(5)	0.8674 (8)	0.2165 (7)	0.8378 (6)	0.046
C(6)	0.7474 (8)	0.2952 (6)	0.9254 (6)	0.036
C(7)	0.6333 (7)	0.4270 (5)	0.6497 (5)	0.029
C(8)	0.4452 (8)	0.3493 (5)	0.6489 (6)	0.035
C(9)	0.5107 (8)	0.4641 (6)	0.7667 (5)	0.036
C(10)	0.5817 (8)	0.2159 (7)	0.5746 (6)	0.041
C(111)	0.9403 (7)	0.2720 (5)	0.6282 (5)	0.030
C(112)	0.9629 (7)	0.3631 (6)	0.6534 (5)	0.031
C(113)	1.0623 (8)	0.3684 (6)	0.7159 (6)	0.043
C(114)	1.1522 (7)	0.3290 (7)	0.6874 (6)	0.045
C(115)	1.1292 (8)	0.2389 (7)	0.6617 (6)	0.045
C(116)	1.0315 (7)	0.2336 (6)	0.5961 (5)	0.035
C(121)	0.7894 (7)	0.3533 (5)	0.4987 (5)	0.029
C(122)	0.6781 (7)	0.3624 (6)	0.4530 (5)	0.032
C(123)	0.6654 (8)	0.4451 (6)	0.4075 (6)	0.041
C(124)	0.7391 (9)	0.4494 (7)	0.3479 (6)	0.053
C(125)	0.8485 (8)	0.4407 (6)	0.3929 (6)	0.043
C(126)	0.8648 (8)	0.3583 (6)	0.4411 (5)	0.038
C(131)	0.8165 (7)	0.1654 (5)	0.5062 (5)	0.027
C(132)	0.8257 (8)	0.0893 (5)	0.5618 (5)	0.036
C(133)	0.8532 (9)	0.0099 (6)	0.5205 (6)	0.049
C(134)	0.7723 (10)	−0.0073 (6)	0.4462 (6)	0.052
C(135)	0.7594 (9)	0.0678 (7)	0.3919 (6)	0.049
C(136)	0.7335 (8)	0.1494 (6)	0.4326 (5)	0.038
H(1)	0.79470	0.31410	0.71520	0.050
H(2)	0.67470	0.39240	0.80680	0.050

[a] $U_{eq} = {}^1/_3\sum_i\sum_j U_{ij}a_i^*a_j^*\mathbf{a}_i\cdot\mathbf{a}_j$.

showed two sharp doublet signals at δ −14.48 (J(P–H) = 7.9, J(Pt–H) = 574 Hz) and −20.66 (J(P–H) = 1.5, J(Pt–H) = 19 Hz), each of relative intensity 1.0, and a weaker doublet at δ −20.20 (J(P–H) = 3.1, J(Pt–H) = 15 Hz) of relative intensity 0.34. The relative proportions of these two sets of signals are essentially constant in all the spectra we have obtained and indicate that complex **3** exists as two isomers (species D and E, see below) in solution, which are interconverting (though not rapidly on the NMR time scale[15]). The major isomer contains inequivalent hydrides bridging an Os–Pt and an Os–Os edge, while the minor isomer contains equivalent hydrides bridging Os–Os edges. The spectroscopic evidence suggests that the major isomer of **3** in solution is related to the red C_1 isomer of **2c**, and this has been confirmed by a single-crystal X-ray study.

(14) Large well-formed crystals of homogeneous color and habit were used. Their poor solubility precluded low-temperature dissolution.

(15) Magnetization transfer studies at 298 K showed a slow exchange between the resonances at δ −14.48 and −20.66, but no detectable exchange between these signals and the one at δ −20.20.

Table II. Selected Bond Lengths (Å) and Bond Angles (deg) for $Os_3Pt(\mu\text{-}H)_2(\mu\text{-}SO_2)(CO)_{10}(PCy_3)$ (3)

Bond Lengths			
Os(1)–Os(2)	2.795 (1)	Os(1)–Os(3)	2.988 (1)
Os(1)–Pt	2.792 (1)	Os(1)–S	2.367 (3)
Os(1)–C(1)	1.943 (12)	Os(1)–C(2)	1.923 (10)
Os(1)–C(3)	1.899 (11)	Os(2)–Os(3)	2.976 (1)
Os(2)–Pt	2.906 (1)	Os(2)–C(4)	1.945 (11)
Os(2)–C(5)	1.912 (12)	Os(2)–C(6)	1.934 (10)
Os(3)–Pt	2.821 (1)	Os(3)–S	2.346 (3)
Os(3)–C(7)	1.964 (9)	Os(3)–C(8)	1.876 (11)
Os(3)–C(9)	1.903 (10)	Pt–P	2.359 (3)
Pt–C(10)	1.847 (11)	S–O(11)	1.444 (7)
S–O(12)	1.475 (8)	O(1)–C(1)	1.114 (15)
O(2)–C(2)	1.143 (13)	O(3)–C(3)	1.140 (14)
O(4)–C(4)	1.115 (14)	O(5)–C(5)	1.115 (15)
O(6)–C(6)	1.115 (12)	O(7)–C(7)	1.141 (12)
O(8)–C(8)	1.151 (13)	O(9)–C(9)	1.116 (12)
O(10)–C(10)	1.152 (14)		
Bond Angles			
Os(2)–Os(1)–Pt	62.7 (1)	Os(2)–Os(1)–S	87.4 (1)
Os(2)–Os(1)–C(1)	162.9 (4)	Os(2)–Os(1)–C(2)	88.1 (3)
Os(2)–Os(1)–C(3)	98.2 (4)	Os(3)–Os(1)–Pt	58.3 (1)
Os(3)–Os(1)–S	50.4 (1)	Os(3)–Os(1)–C(1)	103.4 (4)
Os(3)–Os(1)–C(2)	127.2 (3)	Os(3)–Os(1)–C(3)	131.9 (4)
Pt–Os(1)–S	108.5 (1)	Pt–Os(1)–C(1)	102.9 (4)
Pt–Os(1)–C(2)	69.6 (3)	Pt–Os(1)–C(3)	153.0 (4)
S–Os(1)–C(1)	89.0 (4)	S–Os(1)–C(2)	175.5 (3)
S–Os(1)–C(3)	88.3 (4)	C(1)–Os(1)–C(2)	95.4 (5)
C(1)–Os(1)–C(3)	98.4 (5)	C(2)–Os(1)–C(3)	92.1 (5)
Os(1)–Os(2)–Os(3)	62.3 (1)	Os(1)–Os(2)–Pt	58.6 (1)
Os(1)–Os(2)–C(4)	172.5 (3)	Os(1)–Os(2)–C(5)	93.0 (4)
Os(1)–Os(2)–C(6)	89.5 (3)	Os(3)–Os(2)–Pt	57.3 (1)
Os(3)–Os(2)–C(4)	110.4 (4)	Os(3)–Os(2)–C(5)	150.8 (4)
Os(3)–Os(2)–C(6)	105.2 (3)	Pt–Os(2)–C(4)	117.2 (3)
Pt–Os(2)–C(5)	97.5 (4)	Pt–Os(2)–C(6)	147.6 (3)
C(4)–Os(2)–C(5)	93.8 (5)	C(4)–Os(2)–C(6)	93.9 (5)
C(5)–Os(2)–C(6)	88.8 (5)	Os(1)–Os(3)–Os(2)	55.9 (1)
Os(1)–Os(3)–Pt	57.4 (1)	Os(1)–Os(3)–S	51.0 (1)
Os(1)–Os(3)–C(7)	124.3 (3)	Os(1)–Os(3)–C(8)	97.5 (3)
Os(1)–Os(3)–C(9)	137.8 (3)	Os(2)–Os(3)–Pt	60.1 (1)
Os(2)–Os(3)–S	83.6 (1)	Os(2)–Os(3)–C(7)	92.0 (3)
Os(2)–Os(3)–C(8)	149.7 (3)	Os(2)–Os(3)–C(9)	116.7 (3)
Pt–Os(3)–S	108.1 (1)	Pt–Os(3)–C(7)	67.4 (3)
Pt–Os(3)–C(8)	94.5 (3)	Pt–Os(3)–C(9)	162.0 (3)
S–Os(3)–C(7)	175.0 (3)	S–Os(3)–C(8)	89.9 (3)
S–Os(3)–C(9)	88.4 (3)	C(7)–Os(3)–C(8)	92.7 (4)
C(7)–Os(3)–C(9)	95.8 (4)	C(8)–Os(3)–C(9)	92.5 (5)
Os(1)–Pt–Os(2)	58.7 (1)	Os(1)–Pt–Os(3)	64.3 (1)
Os(1)–Pt–P	150.6 (1)	Os(1)–Pt–C(10)	90.5 (4)
Os(2)–Pt–Os(3)	62.6 (1)	Os(2)–Pt–P	116.0 (1)
Os(2)–Pt–C(10)	147.7 (4)	Os(3)–Pt–P	142.6 (1)
Os(3)–Pt–C(10)	96.9 (4)	P–Pt–C(10)	95.5 (4)
Os(1)–S–Os(3)	78.7 (1)	Os(1)–S–O(11)	118.2 (4)
Os(1)–S–O(12)	113.4 (4)	Os(3)–S–O(11)	116.3 (3)
Os(3)–S–O(12)	112.3 (4)	O(11)–S–O(12)	113.5 (5)
Os(1)–C(1)–O(1)	177.9 (10)	Os(1)–C(2)–O(2)	169.6 (9)
Os(1)–C(3)–O(3)	178.4 (10)	Os(2)–C(4)–O(4)	175.2 (10)
Os(2)–C(5)–O(5)	178.7 (10)	Os(2)–C(6)–O(6)	177.2 (9)
Os(3)–C(7)–O(7)	165.7 (8)	Os(3)–C(8)–O(8)	178.2 (9)
Os(3)–C(9)–O(9)	178.0 (9)	Pt–C(10)–O(10)	177.7 (10)

Crystal Structure of Complex 3. Figure 1 shows the molecular structure and atomic labeling scheme, with a stereoview of the molecule illustrated in Figure 2. Atomic coordinates and important metrical parameters are given in Tables I and II, respectively. The molecular structure of **3** closely resembles that of the C_1 isomer of **2c**,[8] with a μ-SO_2 ligand replacing the μ-CH_2 unit. The tetrahedral Os_3Pt skeleton of the parent cluster **1a**[6] is retained, though consistent with the relief of unsaturation, the Os–Os bond lengths in **3** are slightly greater than the corresponding separations in **1a**. Corresponding Pt–Os distances in **1a** and **3** are, by contrast, rather similar. Metal–metal bond lengths in **3** are very similar to those found[8] in the C_1

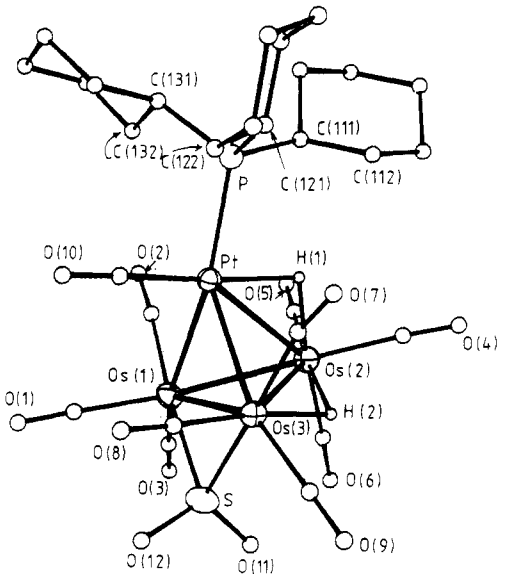

Figure 1. Molecular structure of the complex $Os_3Pt(\mu\text{-}H)_2(\mu\text{-}SO_2)(CO)_{10}(PCy_3)$ (**3**) showing the atomic labeling scheme.

isomer of **2c**, with the exception of the SO_2-bridged Os(1)–Os(3) distance in **3** which is 2.988 (1) Å, while the corresponding CH_2-bridged Os–Os distance in **2c** is 2.865 (1) Å. This difference may be ascribed to the greater steric requirements of the μ-SO_2 ligand versus a μ-CH_2, as has been previously noted[16] in the structural comparison between $Os_3(\mu\text{-}H)_2(\mu\text{-}SO_2)(CO)_{10}$ (**4**)[16] and $Os_3(\mu\text{-}H)_2(\mu\text{-}CH_2)(CO)_{10}$.[17]

Relatively few clusters containing SO_2 ligands have been reported,[16,18-32] with the majority of examples coming from the work of Mingos et al.[23-32] Tetranuclear clusters that have been crystallographically characterized include $Ir_4(\mu\text{-}CO)_2(\mu\text{-}SO_2)(CO)_9$,[21] $Rh_4(\mu\text{-}CO)_4(\mu\text{-}SO_2)(\mu_3\text{-}\eta^2\text{-}SO_2)\{P(OPh)_3\}_4$,[24] $[AuPt_3(\mu\text{-}CO)_2(\mu\text{-}SO_2)(PCy_3)_4]^+$,[27] and $[AuPt_3(\mu\text{-}SO_2)_2(\mu\text{-}Cl)\{P(C_6H_4F)_3\}(PCy_3)_3]^+$.[27] The Rh_4 cluster and the recently reported[31] pentanuclear cluster $Pd_5(\mu\text{-}SO_2)_2(\mu_3\text{-}\eta^2\text{-}SO_2)_2(PMe_3)_5$ are unusual in that they contain μ_3-η^2 S,O 4-electron donor SO_2 ligands. In all other cluster complexes the SO_2 ligands exhibit an η^1 edge-bridging mode, which is somewhat surprising in view of the variety of bonding modes observed in mononuclear SO_2 complexes.[12] The structural parameters involving the SO_2 ligand in **3** are normal. Thus the Os–S distances of 2.367 (3) and 2.346 (3) Å compare well with those found[16] in complex **4** (2.360 (2) and 2.358 (2) Å), and the Os–S–Os angles are also similar (78.7 (1)° in **3** and 75.7 (6)° in **4**[16]). The S atom is virtually coplanar with the Pt–Os(1)–Os(3) triangle (see Figure 2), with a dihedral angle, Pt–Os(1)–Os(3)–S, of 174.2 (1)°. As was observed[8] for the μ-CH_2 complex **2c**, the two carbonyl ligands C(2)–O(2) and C(7)–O(7), which lie in the Pt–Os(1)–Os(3) plane, interact weakly with the Pt atom, such that the associated Pt···C distances are 2.785 (9) and 2.748 (9) Å and the Os–C–O angles 169.6 (9) and 165.7 (8)°, respectively.

Table III. NMR Parameters for Species A[a,c]

reson	chem shift, ppm	mult[b]	assgnt	J, Hz ^{31}P	J, Hz ^{195}Pt	J, Hz H1	J, Hz H2
			^{13}C Data				
a	186.3	d	4/5/6	6.0	55		
b	176.2	d	4/5/6	6.4	*		
c	174.5	d	1	4.3		~5	3.6
d	174.3	s	3			14.0	2.0
e	171.8	s	4/5/6				
f	169.6	s	7/9/10		45		2.0
g	168.3	s	7/9/10				2.9
h	168.1	s	2		*	2.8	8.4
i	167.8	s	7/9/10				2.8
j	167.3	s	8				8.4
			^{1}H Data				
H1	−13.92	dd	Os(μ-H)Pt	7	802		2
H2	−18.94	t	Os(μ-H)Os	2	30	2	
			^{31}P Data				
	69.90	s			4505		

[a] 218 K; CD_2Cl_2. [b] Multiplicities for ^{13}C and ^{31}P based on ^{1}H-decoupled spectra. [c] The asterisk indicates a small resolved ^{195}Pt coupling was expected on the basis of signal intensity but was obscured by overlapping resonances.

The hydride ligands in **3** were not located directly but were included at calculated positions by using the potential energy minimization program HYDEX.[33] These positions are consistent with the metal–metal bond lengths and the carbonyl polytope and agree with the NMR data insofar as one hydride is bridging an Os–Os edge and the other an Os–Pt vector.

NMR Studies on the Reaction of 1a with SO_2 at 195 K. In an attempt to determine the initial site of attack of the SO_2 ligand, we have examined the reaction at low temperatures. Treatment of a solution of **1a** in CD_2Cl_2 at 195 K with an excess of SO_2 rapidly gives rise to a yellow-brown solution. The ^{1}H NMR spectrum of this solution, in the hydride region, is shown in Figure 3. Important ^{1}H, ^{13}C, and ^{31}P NMR parameters for the major (ca. 80% or more) species formed, species A, are given in Table III. The ^{1}H signal at δ −13.92 can be attributed to an Os(μ-H)Pt hydride (H1) from the magnitude of $J(^{195}Pt\text{–}H)$ = 802 Hz, while that at δ −18.94 is due to an Os(μ-H)Os hydride (H2). A small coupling of 2 Hz, which was confirmed as an interhydride H–H coupling by selective decoupling experiments, suggests that the two hydrides are proximate; i.e., they bridge to the same Os atom. Similar small H–H couplings of ~1.5 Hz between the proximate hydrides in $Os_3(\mu\text{-}H)_3(\mu\text{-}CR)(CO)_9$ have been reported.[34] The singlet ^{31}P resonance at δ 69.90 with a

(16) Jarvinen, G. D.; Ryan, R. R. *Organometallics* **1984**, *3*, 1434.
(17) Schultz, A. J.; Williams, J. M.; Calvert, R. B.; Shapley, J. R.; Stucky, G. D. *Inorg. Chem.* **1979**, *18*, 319.
(18) Otsuka, S.; Tatsuno, Y.; Miki, T.; Aoki, M.; Matsumoto, M.; Yoshioka, H.; Nakatsu, K. *J. Chem. Soc., Chem. Commun.* **1973**, 445.
(19) Moody, D. C.; Ryan, R. R. *Inorg. Chem.* **1977**, *16*, 1052.
(20) Browning, C. S.; Farrar, D. H.; Gukathasan, R. R.; Morris, S. A. *Organometallics* **1985**, *4*, 1750.
(21) Braga, D.; Ros, R.; Roulet, R. *J. Organomet. Chem.* **1985**, *286*, C8.
(22) Bogdan, P. L.; Sabat, M.; Sunshine, S. A.; Woodcock, C.; Shriver, D. F. *Inorg. Chem.* **1988**, *27*, 1904.
(23) Mingos, D. M. P.; Wardle, R. W. M. *Transition Met. Chem. (Weinheim, Ger.)* **1985**, *10*, 441.
(24) Briant, C. E.; Theobald, B. R. C.; Mingos, D. M. P. *J. Chem. Soc., Chem. Commun.* **1981**, 963.
(25) Evans, D. G.; Hughes, G. R.; Mingos, D. M. P.; Basset, J.-M.; Welch, A. *J. Chem. Soc., Chem. Commun.* **1980**, 1255.
(26) Hallam, M. F.; Howells, N. D.; Mingos, D. M. P.; Wardle, R. W. M. *J. Chem. Soc., Dalton Trans.* **1985**, 845.
(27) Mingos, D. M. P.; Wardle, R. W. M. *J. Chem. Soc., Dalton Trans.* **1986**, 73.
(28) Briant, C. E.; Evans, D. G.; Mingos, D. M. P. *J. Chem. Soc., Dalton Trans.* **1986**, 1535.
(29) Bott, S. G.; Hallam, M. F.; Ezomo, O. J.; Mingos, D. M. P.; Williams, I. D. *J. Chem. Soc., Dalton Trans.* **1988**, 1461.
(30) Mingos, D. M. P.; Oster, P.; Sherman, D. J. *J. Organomet. Chem.* **1987**, *320*, 257.
(31) Bott, S. G.; Ezomo, O. J.; Mingos, D. M. P. *J. Chem. Soc., Chem. Commun.* **1988**, 1048.
(32) Mingos, D. M. P.; Williams, I. D.; Watson, M. J. *J. Chem. Soc., Dalton Trans.* **1988**, 1509.
(33) Orpen, A. G. *J. Chem. Soc., Dalton Trans.* **1980**, 2509.

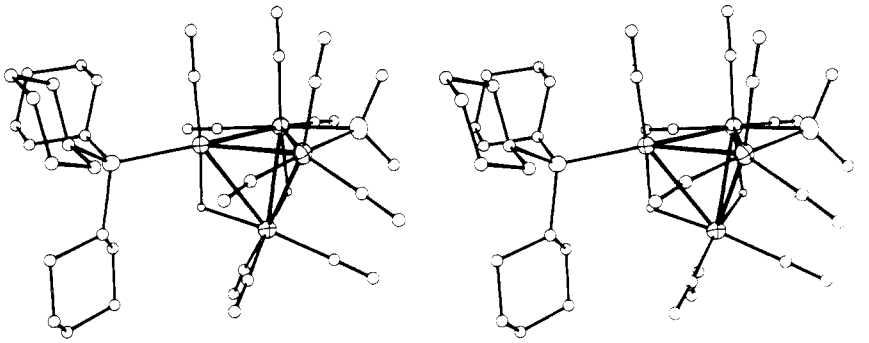

Figure 2. Stereoview of complex 3.

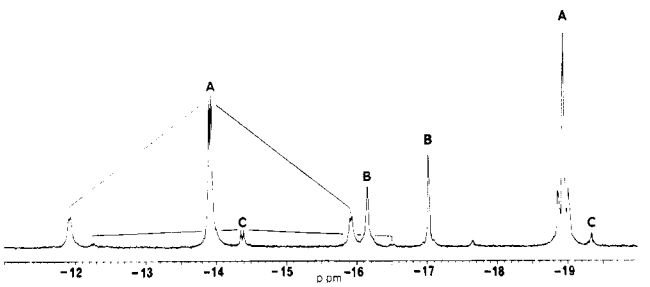

Figure 3. ^1H NMR spectrum (CD_2Cl_2) of the reaction mixture of complex **1a** with SO_2 at 195 K (hydride region).

Table IV. ^1H and ^{31}P Data for Species B–G[a]

	Species B[b]
^1H	δ −16.15 (t, J(P–H) = 1.7, J(H–H) = 1.6, J(Pt–H) = 14 Hz)
	−17.03 (d, J(H–H) = 1.6 Hz)
^{31}P	δ 56.6 (s, J(Pt–P) = 1892 Hz)
	Species C[b]
^1H	δ −14.35 (d, J(P–H) = 8.5, J(Pt–H) = 851 Hz)
	−19.35 (d, J(P–H) = 2.0, J(Pt–H) = 18 Hz)
^{31}P	δ 69.93(s, J(Pt–P) = 4396 Hz)
	Species D[c]
^1H	δ −14.48 (d, J(P–H) = 7.9, J(Pt–H) = 574 Hz)
	−20.66 (d, J(P–H) = 1.5, J(Pt–H) = 19 Hz)
^{31}P	δ 73.0 (s, J(Pt–P) = 2617 Hz)
	Species E[c]
^1H	δ −20.20 (d, J(P–H) = 3.1, J(Pt–H) = 15 Hz)
^{31}P	δ 9.3 (s, J(Pt–P) = 2402 Hz)
	Species F[d]
^1H	δ −15.02 (s)
	−18.15 (s, J(Pt–H) = 28 Hz)
^{31}P	δ 46.2 (s, J(Pt–P) = 2222 Hz)
	Species G[c]
^1H	δ −17.57 (t, J(Pt–H) = 15, J(P–H) = J(H–H) = 1.6 Hz)
	−18.22 (t, J(Pt–H) = 12, J(P–H) = J(H–H) = 1.6 Hz)

[a] CD_2Cl_2. [b] 218 K. [c] 298 K. [d] 233 K.

large ^{195}Pt coupling of 4505 Hz clearly indicates the phosphine ligand remains bonded to the Pt center. The ^{13}C spectrum of a ^{13}CO-enriched sample shows ten signals in the CO region, indicating that species A has low symmetry. The lack of any signal having a large ^{195}Pt coupling is of particular relevance, since this clearly indicates that there is *no Pt-bound carbonyl* in species A. For CO ligands directly bonded to Pt in Os_3Pt clusters typical values for $^1J(^{195}Pt–C)$ are 1500–1750 Hz.[9,11] We hence presume that there is an SO_2 ligand coordinated to the Pt center.

While the spectroscopic data do not unambiguously allow assignment of the structure of species A, several points are clear. The $^1H–^{13}C$ coupling constants (Table III) show that seven CO ligands (resonances c, d, and f–j) are coupled to H2 (at δ −18.94), with three of these signals (c, d, and h) also coupled to H1 (at δ −13.92). This indicates that the Os(μ-H)Os hydride H2 bridges between an $Os(CO)_3$ group and an $Os(CO)_4$ group, while the Os(μ-H)Pt hydride H1 bridges from the Pt atom to the same $Os(CO)_3$ unit. Three CO resonances a, b, and e show no coupling to either hydride and are presumably due to an $Os(CO)_3$ group more remote from the hydrides. The structure shown is compatible with the data, though the exact bonding mode of the SO_2 ligand remains unclear. Due to the instability of species A, we have been unable to obtain IR data on the S–O stretching bands which might prove informative. Either terminal or bridging modes (including μ_x-η^2-S,O) are likely, though we cannot discount the possibility that A contains more than one SO_2 ligand. The polarization of the SO_2 molecule, i.e. $S^{\delta 2+}(O^{\delta -})_2$[35] suggests (in conjunction with charges for **1** obtained from EHMO calculations) that if a μ_x-η^2-S,O mode is present in species A–C, it is likely that the Pt atom is O-bonded and an Os atom is S-bonded.

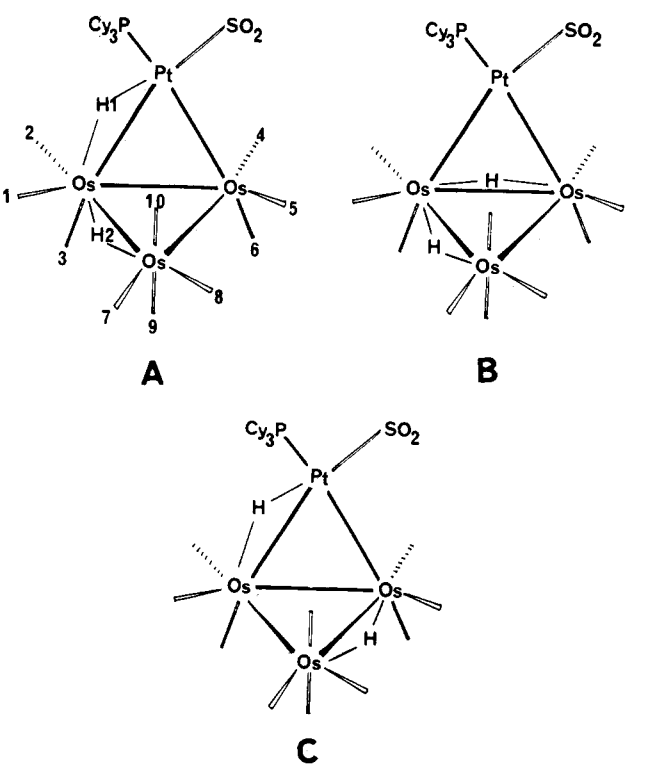

(34) Holmgren, J. S.; Shapley, J. R.; Belmonte, P. A. *J. Organomet. Chem.* **1985**, *284*, C5.

(35) Our EHMO calculations place a charge of +0.98 on the S atom; Xα–SW calculations produce a similar charge of +1.15, see: Noodleman, L.; Mitchell, K. A. R. *Inorg. Chem.* **1978**, *17*, 2709.

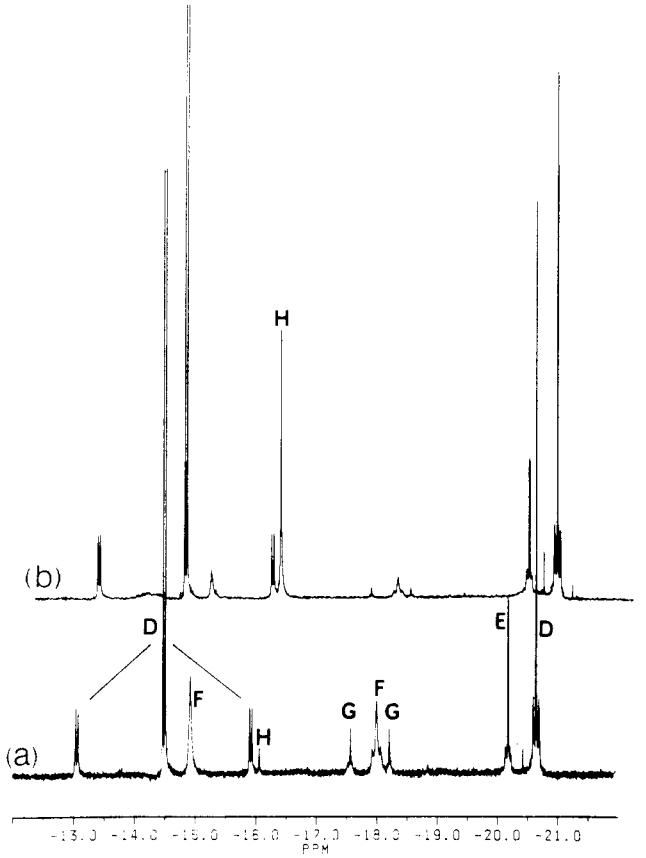

Figure 4. ^1H NMR spectrum (CD_2Cl_2) of the reaction mixture of complex **1a** with SO_2 at 298 K (hydride region): (a) ca. 0.5 h after addition of SO_2; (b) same solution as (a) after 12 h. The upper spectrum has been shifted slightly for clarity.

In addition to species A, two other complexes are also formed at 195 K, species B in ca. 10–20% yield with hydride resonances at δ −16.15 and −17.03 and a ^{31}P signal at δ 56.6 and smaller quantities of species C with hydride signals at δ −14.35 and −19.35 and a ^{31}P signal at δ 69.93. Further details, given in Table IV, clearly show from the large ^{31}P–^{195}Pt couplings that both complexes have Pt-bound phosphine ligands. Species B has two inequivalent Os(μ-H)Os groups with a small H–H coupling suggesting they are proximate, while the NMR parameters for species C closely resemble those of A. The suggested structures are compatible with the data, though by no means unique.

NMR Studies of the Reaction of 1a with SO_2 at 298 K. If the solution prepared at 195 K is allowed to warm to 298 K, there is a rapid and irreversible color change from yellow-brown to red. ^1H NMR spectra of this solution are essentially the same as those obtained from direct reaction of **1a** with SO_2 at 298 K. The spectum obtained from the direct reaction is shown in Figure 4a. Signals due to species A–C disappear rapidly on warming, and resonances from five new species D–H become visible. NMR details for D–G are given in Table IV. Spectra obtained during the warming process show that species A is rapidly converted to B, which then more slowly converts to the mixture shown in Figure 4a. The major component at 298 K, species D, is assigned to the isolated complex **3**, and the signal from the isomeric species E at δ −20.20 is also observed. The spectra are both time and temperature dependent, and the spectrum obtained after 12 h is shown in Figure 4b. Signals from species F and G slowly diminish in intensity with time, while that due to H increases. If the excess SO_2 is removed, then the signal at δ −16.06 due to H increases in intensity more rapdily, such that after 12 h this compound is the predominant hydride-containing species. The removal of the SO_2 also results in significant amounts of the known[7,8] complex $Os_3Pt(\mu\text{-}H)_2(CO)_{11}(PCy_3)$ (**5**), as evidenced by ^1H signals at δ −11.44 and −17.56 and a ^{31}P resonance at δ 50.8. This complex presumably arises from loss of SO_2 from **3**, followed by addition of adventitious CO.

A solution of a pure crystalline sample of complex **3** in CD_2Cl_2 saturated with SO_2 gave a very similar spectrum after 12 h to that shown in Figure 4b. A similarly prepared solution containing *no* added SO_2 showed strong signals due to **5** but was otherwise the same. These results indicate that the isolated complex **3** is unstable in solution, particularly in the absence of excess SO_2, and that there is a complex set of equilibria relating several species, which is dependent on the SO_2 concentration. Unfortunately this mixture could not be separated by column chromatography, and we have only been able to obtain solution NMR data. The relationships between the various ^1H and ^{31}P resonances were established by selective decoupling and saturation experiments and by consideration of relative intensities in the time dependent spectra.

Evidence for Dynamic Behavior. Theoretical studies[36] have suggested that the barrier to rotation of the PtL_2 unit about the M_3 centroid in tetrahedral M_3Pt clusters could be very low. We have reported[11] that the variable-temperature ^{13}C spectra of complex **1a** and $[Os_3Pt(\mu\text{-}H)_3(CO)_{10}(PCy_3)]^+$ are compatible with such a process and have recently obtained[37] unequivocal evidence for the "spinning" of the $Pt(H)(CNCy)(PCy_3)$ in $Os_3Pt(\mu\text{-}H)_2(CO)_9(CNCy)(PCy_3)$ from dynamic ^{187}Os–H couplings. The barrier to rotation of the $Pt(CO)_2$ unit in $[Pt_4(\mu_3\text{-}CO)(CO)_2(\eta\text{-}C_5Me_5)_3]^+$ is also apparently very low.[38] Such dynamic processes must therefore be considered for the isomers of $Os_3Pt(\mu\text{-}H)_2(\mu\text{-}SO_2)(CO)_{10}(PCy_3)$ (**3**). The rotation of the PtL_n unit in **3** is not a degenerate process, and Chart II shows there are three possible[39] C_1 rotomers having one Os(μ-H)Os and one Os(μ-H)Pt hydride, rotomers a–c, and four rotomers having two Os(μ-H)Os hydrides, rotomers d–g. Rotomers e and g have enantiomeric pairs and inequivalent hydrides, while the C_s rotomers d and f have equivalent hydride ligands. Free rotation of the PtL_n unit will result in interchange of rotomers a–c with each other, and rotomers d–g with each other, but extra fluxional processes are necessary to exchange isomers between these two groups.

At 298 K the major solution species D (which from the crystal structure we assume corresponds to rotomer b, Chart II) shows ten sharp CO resonances in the ^{13}C NMR spectrum (see Experimental Section). Individual assignments were not possible, apart from the signal at δ 159.3 which has a ^{195}Pt coupling of 1560 Hz and can be clearly assigned to the carbonyl C(10) on the Pt atom. This resonance is also coupled to the Pt(μ-H)Os hydride (J(H–C) = 33 Hz). The ^{187}Os satellite patterns seen on the hydride signals of D are compatible with rigidity of the cluster framework. Figure 5a shows that two satellite sets ($J(^{187}Os\text{–}H)$ = 40.7, 32.0 Hz) are observed for the Os(μ-H)Os signal, due to coupling to the inequivalent Os atoms

(36) Schilling, B. E. R.; Hoffmann, R. *J. Am. Chem. Soc.* **1979**, *101*, 3456.
(37) Farrugia, L. J., submitted for publication.
(38) Boag, N. M., personal communication. See also: Boag, N. M. *J. Chem. Soc., Chem. Commun.* **1988**, 617.
(39) The Pt-bound ligand (PR_3 or CO) eclipsing the Pt–Os edge is not shown. We have only considered those rotomers with the plane of the PtL_n unit *perpendicular* to an Os–Os vector since theoretical studies[36] indicate that configurations with a *parallel* geometry are at energy maxima. In addition only those configurations with the phosphine cis to the Pt(μ-H)Os hydride are considered sterically favorable: see ref 8.

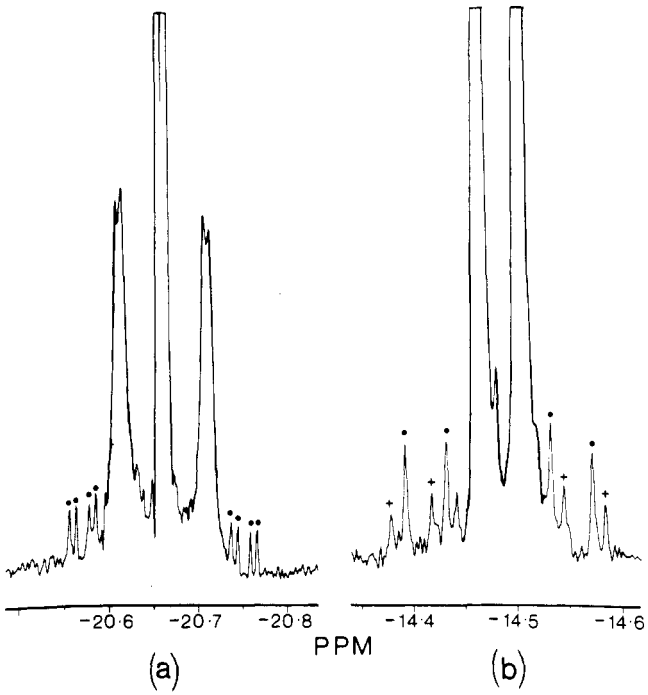

Figure 5. Expansions in the hydride region of ^1H NMR signals due to complex **3** (species D): (a) the Os(μ-H)Os signal, showing the ^{187}Os (·) and ^{195}Pt satellites; (b) the Os(μ-H)Pt signal, showing the ^{187}Os (·) and ^{13}C (+) satellites.

Chart II

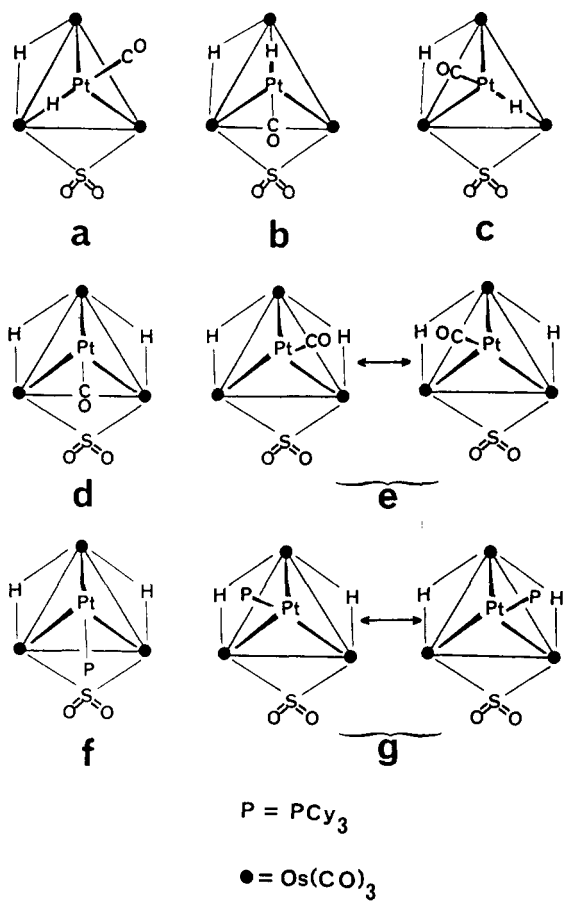

Os(2) and Os(3). As expected only one ^{187}Os–H coupling (28.1 Hz) is observed[40] for the Os(μ-H)Pt signal (Figure 5b). These magnitudes fall within the range reported in the literature for nondynamic $^1J(^{187}Os–H)$ couplings in hydridoosmium clusters.[34,41] However both the hydride and ^{31}P signals due to species D broaden at 168 K, which implies that a fluxional exchange is being frozen out at this temperature. The origin of this behavior is not clear, but if it arises from the slowing of a rapid exchange between rotomers a, b, and c caused by a rotation of the Pt(H)(CO)(PCy_3) unit, then the ^{187}Os couplings observed at 298 K are only compatible with such an exchange if we assume one rotomer predominates at this temperature. This follows since rapid rotation does not introduce a new time-averaged symmetry element, and hence at the fast-exchange regime each hydride and carbonyl resonance will occur at population-weighted chemical shifts and display population-weighted coupling constants.

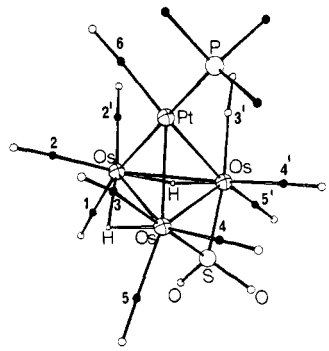

Figure 6. The proposed structure of species E and complex **6** (major isomer).

Species E shows a single Os(μ-H)Os resonance at δ −20.20 and a ^{31}P signal at δ 9.3. These chemical shifts (and the ^{31}P and ^{195}Pt couplings, Table IV) are very similar to those assigned to the yellow C_s isomer of **2a**[8] (ii, Chart I), and hence we propose for E the structure shown in Figure 6 (corresponding to rotomer f). The hydride signal broadens considerably on cooling below 178 K, though the ^{31}P resonance remains sharp, indicating the freezing out of fluxional processes, which may possibly involve a rotation between rotomers d–g.[42]

Relatively little can be said about species F and G, save that they both have two inequivalent Os(μ-H)Os hydrides and one $PtPCy_3$ unit. Since their formation is unaffected by the presence or absence of SO_2 but is supressed under a CO atmosphere, we suspect they arise from loss of CO from isomers of **3**. They may possibly contain μ_3-η^2-SO SO_2 ligands. Variable-temperature spectra show that the broad hydride signals attributed to species F at 298 K (Figure 4a) arise from a rapid nondegenerate exchange between at least two isomers. The broadening seen at 298 K is due to exchange between the inequivalent hydride environments, as shown by saturation transfer experiments. On cooling to 218 K these signals sharpen due to the slowing of this exchange but on further cooling broaden again and decoalesce at 168 K. The signal at δ −15.02 splits into two signals at δ −15.08 and −15.18 (intensity ratio 0.1:0.9), as does the signal at δ −18.15, giving resonances at δ −18.15 and −18.20 (intensity ratio 0.1:0.9). The ^{31}P

(40) In addition a ^{13}C–^1H coupling of 33 Hz, also observed in the ^{13}C spectrum, is clearly resolved.

(41) (a) Constable, E. C.; Johnson, B. F. G.; Lewis, J.; Pain, G. N.; Taylor, M. J. *J. Chem. Soc., Chem. Commun.* **1982**, 754. (b) Koridze, A. A.; Kizas, O. A.; Kolobova, N. E.; Petrovskii, P. V.; Fedin, E. I. *J. Organomet. Chem.* **1984**, *265*, C33. (c) Colbran, S. B.; Johnson, B. F. G.; Lahoz, F. J.; Lewis, J.; Raithby, P. R. *J. Chem. Soc., Dalton Trans.* **1988**, 1199.

(42) A hindered rotation of the Pt(CO)(PR_3) resulting in an exchange between either the enantiomers of rotomer e or those of rotomer g would account for the observed behavior, since this process exchanges the two inequivalent hydrides but has no effect on the P environment.

spectrum shows a corresponding behavior, with the signal at δ 46.2 broadening below 218 K and decoalescing at 168 K to two signals at δ 44.9 (J(Pt–P) = 2243 Hz) and 45.7 (J(Pt–P) = 2197 Hz) with relative intensities 0.1:0.9, respectively.

Cluster Degradation Reactions. Cluster degradation is a major reaction pathway for complex **3** in the absence of high concentrations of SO_2. Species H becomes the predominant hydride-containing species under these conditions. The singlet hydride resonance (δ −16.06) for H at 298 K collapses to two doublets at δ −16.05 and −16.14 (J(H–H) = 1.4 Hz) on cooling to 213 K, indicating that species H contains inequivalent hydrides that undergo exchange. Although we have not isolated pure H, a ^{13}C spectrum at 198 K of a mixture containing ca. 50% of this species shows nine sharp CO signals of equal intensity from δ 176.4 to δ 158.1 that can unambiguously be assigned to H on the basis of selective ^1H decoupling experiments. These signals show no evidence of ^{31}P or ^{195}Pt couplings and indicate that species H does not contain a $PtPCy_3$ unit. As mentioned below ^1H signals for species H are also seen when the reaction mixture of **1b** (the triphenylphosphine analogue of **1a**) and SO_2 is allowed to stand, which is further evidence for the lack of a $PtPR_3$ unit in H. The NMR data (see Experimental Section) suggest a formulation $Os_3(\mu\text{-}H)_2(CO)_9(SO_2)_n$ (n = 1 or 2) for species H. Jarvinen and Ryan[16] have reported the synthesis and structure of $Os_3(\mu\text{-}H)_2(\mu\text{-}SO_2)(CO)_{10}$, which is formed by reaction of $Os_3(\mu\text{-}H)_2(CO)_{10}$ with SO_2. We have reexamined this reaction and concur with the findings of these authors in that numerous other hydride-containing products are also formed. However no significant signals attributable to species H were observed. Solutions containing significant concentrations of species H show in addition a ^{31}P signal at δ 68.5 due to another species, with ^{195}Pt couplings (J(Pt–P) = 4056, 330; J(P–P) = 34 Hz) characteristic of a complex containing two equivalent $Pt(PCy_3)$ units. This signal may arise from a symmetric Pt_2 species[43] or a Pt_2Os_n cluster resulting from degradation of the starting Os_3Pt cluster. Small quantities of the known cluster $Pt_3(\mu\text{-}SO_2)_2(\mu\text{-}CO)(PCy_3)_3$ were also isolated and identified by a single-crystal X-ray structure.[45]

Reaction of Complex 1b with SO_2. Although we have not followed the reaction of (**1b**, R = Ph) with SO_2 in as much detail, NMR studies show that a similar reaction ensues, but the relative stabilities of the various isomers and complexes are strikingly different. The major species formed (ca. 90%) has been isolated as yellow microcrystals and characterized as $Os_3Pt(\mu\text{-}H)_2(\mu\text{-}SO_2)(CO)_{10}(PPh_3)$ (**6**). NMR parameters for this complex are given in Table V. Complex **6** appears to be more stable in solution than complex **3** and shows a single hydride resonance at δ −20.27 indicative of two equivalent $Os(\mu\text{-}H)Os$ protons. The ^{13}C spectrum in the CO region is consistent with C_s symmetry, and we assign a structure, shown in Figure 6, similar to that for species E and analogous to the C_s isomer of **2c**. The relatively large ^{31}P coupling of 17.4 Hz on the CO resonance at δ 168.8 is consistent with a trans disposition of the phosphine relative to the unique carbonyl C1 on Os.[46] Despite numerous attempts no crystals suitable for an X-ray determination could be obtained. The other principal species formed (ca. 10%) shows one doublet resonance at δ −20.15 (J(P–H) = 3.3, J(Pt–H) = 15.5 Hz) in the hydride region and a singlet in the ^{31}P spectrum at δ 20.7 (J(Pt–P) = 3540 Hz) and may be a rotomer of **6**, though there is no evidence for any exchange between these species.

Only trace amounts of hydride signals were observed that could be attributable to analogues of the cyclohexylphosphine species D [resonances at δ −13.06 (J(P–H) = 10.3, J(Pt–H) = 573 Hz) and δ −20.95 (J(P–H) = 1.5, J(Pt–H) = 18 Hz)] and species F [resonances at δ −14.91 and −18.00 (J(P–H) = 2, J(Pt–H) = 29 Hz)]. A signal at δ −16.06 attributed to species H was also observed. The substituents on the phosphine ligand (and hence its steric and electronic factors) thus have a significant effect on the relative stabilities of the C_1 versus the C_s isomers of the SO_2 adducts of complex **1**.

Table V. NMR Parameters for $Os_3Pt(\mu\text{-}H)_2(\mu\text{-}SO_2)(CO)_{10}(PPh_3)$ (Major Isomer)[a]

chem shift, ppm	mult[b]	assgnt[c]	J, Hz ^{31}P	^{195}Pt	^1H
		^{13}C Data			
178.6 (2)[d]	d	C3/C5	1.8	56	
174.5 (2)	s	C3/C5			4
174.0 (1)	d	C6	17.1	1790	
168.8 (1)	d	C1	17.4		4
167.2 (2)	d	C2/C4	3.1		10
163.4 (2)	s	C2/C4			11
		^1H Data			
−20.27	d	$Os(\mu\text{-}H)Os$	3.2	15	
		^{31}P Data			
−10.1	s	Pt–P		2499	

[a] 298 K; CD_2Cl_2. [b] Multiplicities for ^{13}C and ^{31}P based on ^1H-decoupled spectra. [c] See Figure 6. [d] Relative intensities in parentheses.

Conclusions

Although the reaction of complex **1a** with SO_2 affords thermodynamic products analogous to those obtained with CH_2N_2, the reaction pathway is complex and other species are formed. The initial kinetic product appears to involve attack by SO_2 at the platinum center, combined with a migration of a CO ligand from Pt to Os, yielding a butterfly species. The apparent migration of a Pt bound ligand has been previously observed[9] in the reaction of the related cluster $Os_3Pt(\mu\text{-}H)_2(CO)_9(CNCy)(PCy_3)$ with CO, where the isonitrile ligand moves from Pt to Os on formation of the butterfly adduct. The experimental results disagree with our predictions based on EHMO calculations on complex **1**, which suggest that attack by SO_2 should proceed at the Os centers, irrespective of whether orbital or charge control is operative.

Experimental Section

All manipulations were carried out under dry, oxygen-free dinitrogen atmosphere, using standard vacuum line/Schlenk tube techniques. Solvents were deoxygenated and freshly distilled under dinitrogen prior to use; petroleum ether refers to that fraction with a boiling point of 40–60 °C. ^1H, ^{13}C, and ^{31}P NMR spectra were obtained on a Bruker WP 200SY FT NMR spectrometer. Chemical shifts were referenced to internal solvent signals for ^1H and ^{13}C spectra and are reported relative to Me_4Si.

(43) These signals are not due to the known[44] complex $Pt_2(\mu\text{-}SO_2)(CO)_2(PCy_3)_2$.

(44) Evans, D. G.; Hallam, M. F.; Mingos, D. M. P.; Wardle, R. W. M. *J. Chem. Soc., Dalton Trans.* **1987**, 1889.

(45) Crystal data: monoclinic; space group $P2_1/n$; a = 15.362 (2), b = 21.653 (13), c = 20.881 (5) Å; β = 86.64 (2)°; V = 6933 (5) Å^3; Z = 4; current R (R_w) = 0.079 (0.107) for 3402 independent, absorption-corrected, observed ($I > 2.0\sigma(I)$) data. This complex has also been structurally characterized by D. M. P. Mingos and co-workers (personal communication).

(46) Relatively large $^3J(^{13}C\text{–}^{31}P)$ coupling constants across metal–metal bonds have been previously reported in cases where the phosphine and CO ligands are in a transoid geometry; see, for example: Stuntz, G. F.; Shapley, J. R. *J. Am. Chem. Soc.* **1977**, *99*, 607.

Table VI. Experimental Data for Crystallographic Study

formula	$C_{28}H_{35}O_{12}Os_3PPtS$
M_r	1392.3
space group	$P2_1/n$ (No. 14, C_{2h}^5)
cryst system	monoclinic
a, Å	13.254 (2)
b, Å	15.893 (5)
c, Å	17.079 (2)
β, deg	101.073 (9)
V, Å^3	3531 (1)
Z	4
D_{calcd}, g cm^{-3}	2.62
$F(000)$	2544
μ(Mo Kα), cm^{-1}	149.0
T, K	298
scan mode	$\theta/2\theta$
θ range, deg	$2 < \theta < 25$
cryst size, mm	0.18 × 0.38 × 0.38
range of trans coeff corr	0.77/1.65
no. of data collected	6751
no. of unique data	6204
std reflctns	814, 148, 457
observability criterion n ($I > n\sigma(I)$)	3.0
no. of data in refinement	4622
no. of refined parameters	253/217
final R	0.027
R_w	0.036
largest remaining feature in elec density map, e Å^3	+1.47 (max), −1.26 (min)
shift/esd in last cycle	0.16 (max), 0.03 (av)

^{31}P spectra were referenced to external 85% H_3PO_4. Infrared spectra were measured on a Perkin-Elmer 983 photospectrometer. Elemental analyses (C/H) were performed by the microanalytical unit in the Department of Chemistry, University of Glasgow. Sulfur dioxide (BDH) was used as supplied, and $Os_3Pt(\mu\text{-}H)_2(CO)_{10}(PR_3)$ (R = Cy, Ph) was prepared as previously described.[6]

Preparation of $Os_3Pt(\mu\text{-}H)_2(\mu\text{-}SO_2)(CO)_{10}(PCy_3)$ (3). A solution of $Os_3Pt(\mu\text{-}H)_2(CO)_{10}(PCy_3)$ (0.2 g, 0.15 mmol) in CH_2Cl_2 (5 mL) was saturated with SO_2 by rapid passage of the gas and the solution allowed to stand for 0.5 h. Light petroleum (ca. 5 mL) was added and the solution stored at −20 °C overnight. Large well-formed dark red crystals of the product $Os_3Pt(\mu\text{-}H)_2(\mu\text{-}SO_2)(CO)_{10}(PCy_3)$ are obtained (0.11 g, 0.08 mmol, 53% yield): IR (KBr disk) ν_{CO} 2100 (w), 2080 (vs), 2060 (s), 2040 (s), 2018 (s), 1995 (m), 1985 (s), 1956 (m), ν_{SO} 1195 (vw), 1040 (s) cm^{-1}; ^{1}H and ^{31}P NMR, see text; ^{13}C NMR (CD_2Cl_2, 298 K, CO region, ^{13}CO-enriched sample) δ 179.4 (d, 1 C, J(P–C) = 8.0 Hz), 176.8 (s, 1 C), 174.2 (d, 1 C, J(P–C) = 8.4 Hz), 172.8 (s, 1 C), 172.2 (s, 1 C), 172.17 (s, 1 C), 172.0 (s, 1 C), 169.5 (s, 1 C, J(Pt–C) = 28 Hz), 161.7 (d, 1 C, J(P–C) = 1.3, J(H–C) = 12 Hz), 159.3 (d, 1 C, J(P–C) = 6.3, J(Pt–C) = 1560, J(H–C) = 33 Hz). Anal. Calcd for $C_{28}H_{35}O_{12}Os_3PtPS$: C, 24.15; H, 2.53. Found: C, 24.33; H, 2.31.

NMR Data for Species H: ^{1}H NMR (CD_2Cl_2, 213 K) δ −16.05 (d, H1, J(H–H) = 1.4 Hz), −16.14 (d, H2, J(H–H) = 1.4 Hz); ^{13}C (CD_2Cl_2, 198 K, ^{13}CO-enriched sample, CO region) δ 176.4 (J(H2–C) = 10.3 Hz), 175.3 (J(H1–C) = 4.8 Hz), 174.3 (J(H1–C) = 7.3 Hz), 171.9 (J(H2–C) = 3.0 Hz), 169.6 (J(H2–C) = 3.4 Hz), 166.7 (J(H1–C) = 4.6, J(H2–C) = 4.6 Hz), 164.2 (J(H1–C) = 2.2 Hz), 163.8 (J(H1–C) = 10.2, J(H2–C) = 4.7 Hz), 158.1 (J(H1–C) = 3.8, J(H2–C) = 11.7 Hz).

Preparation of $Os_3Pt(\mu\text{-}H)_2(\mu\text{-}SO_2)(CO)_{10}(PPh_3)$ (6). Treatment of 0.2 g (0.16 mmol) of complex **1b** with SO_2 and similar workup to complex **3** afforded bright yellow microcrystals of complex **6** (0.16 g, 0.12 mmol, 75% yield): IR (CH_2Cl_2) ν_{CO} 2105 (s), 2084 (vs), 2070 (vs), 2038 (vs), 2027 (vs), 1971 (m) cm^{-1}; IR (KBr disk) ν_{SO} 1208 (w), 1055 (s) cm^{-1}; NMR data, see text. Anal. Calcd for $C_{28}H_{17}O_{12}Os_3PPtS$: C, 24.47; H, 1.25. Found: C, 24.89; H, 0.82.

Crystal Structure Determination. Details of data collection procedures and structure refinement are given in Table VI. Data were collected on an Enraf-Nonius CAD4F automated diffractometer, with graphite-monochromated X-radiation (λ = 0.71069 Å). Unit cell parameters were determined by refinement of the setting angles ($\theta \geq 12°$) of 25 reflections. Standard reflections were measured every 2 h during data collection, and a decay corresponding to 4% over 10000 reflections was observed and corrected for. Lorentz–polarization and absorption (DIFABS[47]) corrections were also applied. Systematic absences uniquely determined the space group $P2_1/n$. The structure was solved by direct methods (MITHRIL[48]) and subsequent electron density difference syntheses. All non-hydrogen atoms were allowed anisotropic thermal motion. Hydride positions were determined from potential energy minimization calculations (HYDEX,[33] Os–H, Pt–H = ca. 1.85 Å), while cyclohexyl hydrogens were included at calculated positions (C–H = 1.073 Å). Isotropic thermal parameters for H atoms were fixed at 0.05 Å^2. Refinement was by full-matrix least squares, but due to matrix size limitations the parameters were divided into two blocks (253, 217) and each was refined separately. The function minimized was $\sum w(|F_o| - |F_c|)^2$ with the weighting scheme $w = [\sigma^2(F_o)]^{-1}$ used and judged satisfactory. $\sigma(F_o)$ was estimated from counting statistics. Neutral atom scattering factors were taken from ref 49 with corrections for anomalous dispersion. All calculations were carried out on a Gould-SEL 32/27 mini computer using the GX suite of programs.[50]

Acknowledgment. We thank the SERC for a research studentship to P.E. and Johnson-Matthey for a generous loan of Pt salts.

Registry No. **1a**, 68091-56-5; **1b**, 68091-55-4; **3**, 120204-16-2; **5**, 77700-90-4; **6**, 120204-17-3; SO_2, 7446-09-5; Pt, 7440-06-4; Os, 7440-04-2.

Supplementary Material Available: Tables of anisotropic thermal parameters and calculated hydrogen positional parameters and a complete listing of bond lengths and angles (6 pages); listings of calculated and observed structure factors (22 pages). Ordering information is given on any masthead page.

(47) Walker, N.; Stuart, D. *Acta Crystallogr., Sect. A: Found. Crystallogr.* **1983**, *A39*, 158.
(48) Gilmore, C. J. *J. Appl. Cryst.* **1984**, *17*, 42.
(49) *International Tables for X-Ray Crystallography*; Kynoch: Birmingham, 1974; Vol. 4.
(50) Mallinson, P. R.; Muir, K. W. *J. Appl. Cryst.* **1985**, *18*, 51.